Clays and Clay Minerals, Vol. 41, No. 5, 631–634, 1993.

NOTE

REINTERPRETATION OF THE X-RAY DIFFRACTION PATTERNS OF STICHTITE AND REEVESITE

Key Words—Hydrotalcite-like minerals, Polytype, Reevesite, Stichtite, X-ray diffraction.

INTRODUCTION

Stichtite and reevesite are built of positively charged brucite-like layers and contain charge-compensating CO_3^{2-} anions and water molecules in interlayers, which identify them as members of the hydrotalcite-like group of minerals. In the literature, authors have failed to agree about stichtite and reevesite polytypism. White *et al.* (1967) described reevesite and Taylor (1973) described stichtite in terms of a three-layer rhombohedral cell with a = 3 Å. De Waal and Viljoen (1971) found additional reflections in the XRD pattern of reevesite and proposed a new cell with a doubled a-parameter and number of layers. For the same reason, the XRD data of stichtite given in ASTM card (PDF) # 14-330 and reported by Tatarinov *et al.* (1985) was also interpreted in terms of a similar double cell. The present work is a further study of stichtite and reevesite polytypism in an attempt to clarify whether six-layer polytypes of hydrotalcite-like minerals exist.

MATERIAL AND EXPERIMENTS

A sample of stichtite from an ophiolite zone on Terectin Ridge (Altai Mountains) originally studied by Tatarinov *et al.* (1985) was kindly provided by the authors. The sample was a mixture of pink and greenish grains. As noted by Tatarinov *et al.* (1985), the pink grains changed their color to green when exposed to light or X-rays. The chemical composition of the sample is presented in Table 1 as reported by Tatarinov *et al.* (1985). Using a binocular microscope, the sample was divided into fractions of two colors. XRD data were recorded on a DRON-4 automatic powder diffractometer using graphite filtered CuKα radiation at 1°(2θ)/min for both oriented and random powder specimens. The experimental data for reevesite were obtained from De Waal and Viljoen (1971).

RESULTS AND DISCUSSION

The X-ray diagram from an oriented specimen is characterized by a rational series of basal reflections with an interlayer distance c_0 = 7.76 Å for the pink grains and with c_0 = 7.37 Å for the greenish grains (Figure 1). Also included in Figure 1 is an XRD pattern of a pink specimen exposed to light for one week. The XRD pattern of the pink grains (Figure 1A) contains a set of narrow *hkl* reflections. Positions of all reflections fit a three-layer rhombohedral cell, common for most hydrotalcite-like CO_3^{2-}-bearing minerals. The unit cell parameters, experimental and calculated peak positions, and their indices are shown in Table 1.

To test the crystal structure of the mineral, we have simulated its powder XRD pattern. A refined structure of hydrotalcite (Allmann and Jepsen, 1969) was used as the structure model. Good agreement between strong, moderate, and weak reflections in the calculated and experimental pattern (Table 2) suggests that the pink crystals are isostructural with hydrotalcite $3R_1$ (notation proposed by Bookin and Drits, 1993, which allows us to apply the name stichtite to them.

The greenish sample has an XRD pattern that can be indexed in terms of a one-layer (1H) hexagonal cell with a = 5.30 Å and c = 7.36 Å (Table 2). In contrast to basal reflections, the non-basal reflections are rather broad, and *hk0* reflections (e.g., *100* and *210*) have shapes typical of two-dimensional diffraction bands (Figure 1C).

The XRD diagram of a pink sample that was exposed to light for one week (Figure 1B) has features of both patterns. It contains split basal reflections with interlayer distances matching those for pink and greenish grains. Parts of non-basal peaks are consistent with a rhombohedral cell of stichtite, and other parts resemble the X-ray diagram of the greenish grains. In fact, depending on the exposure time and light or X-ray intensity, different proportions of the coexisting phases can be obtained. These results suggest that the greenish grains represent an end-member product of a structural transformation of stichtite. Hereafter we will refer to this phase as "modified stichtite."

Three processes are postulated to occur during stichtite transformation. The first involves regular displacement of layers in $3R_1$ stichtite along the $[\bar{1}10]$ direction, resulting in 1H polytype stacking. The second process is shrinking of the interlayer distance by 0.4 Å. This shrinking happens abruptly, for a series of experiments with light-exposed samples showed neither mixed-layer phenomena nor intermediate d-spacings. The last

Table 1. Chemical composition of the stichtite sample.

Oxide	MgO	MnO	CaO	Cr_2O_3	Fe_2O_3	Al_2O_3	SiO_2	CO_3	H_2O
Wt. %	37.30	0.03	0.10	14.38	2.90	3.80	2.18	9.46	29.68

process is the development of a supercell in the *ab* plane, probably through ordering of either CO_3^{2-} in the interlayers or cations in layers over the nodes of a lattice with $a = \sqrt{3}a_0$. The two-dimensional form of the *hk0* bands may be due to the fact that the ordering is not repeated strictly along the *c* axis.

In the light of the results described above, we can give a new interpretation for the XRD data of stichtite given in the ASTM (PDF) card # 14-330. Of the six diffraction peaks, incompatible with the hydrotalcite-like rhombohedral cell, only one additional reflection was indexed in the double unit cell. Peaks at 7.2 Å, 3.62 Å, and 2.50 Å were attributed to the admixture of serpentine, and peaks at 4.30 Å and 1.84 Å were left unexplained. In fact, the set of *d*-values and peak intensities is very similar to that of light exposed stichtite, suggesting that the sample is in an intermediate stage of the stichtite transformation. All of the reflections on ASTM (PDF) card # 14-330 can be interpreted as resulting from a mixture of $3R_1$ stichtite proper and 1H modified stichtite (Table 3). Some observed reflections (e.g., those at 2.6 Å, 1.66 Å, 1.54 Å, and others) may belong to both phases, but in Table 3 we have assigned indices of a 1H cell only to those peaks that cannot be indexed in a rhombohedral cell.

The XRD data of reevesite (De Waal and Viljoen, 1971) can be interpreted in a similar way. The most intense reflections fit the unit cell of the $3R_1$ polytype. Among reflections inconsistent with a rhombohedral cell are peaks at $d = 7.2$ Å, 4.6 Å, and 3.6 Å (Table 4) that have been observed in the X-ray diagram of modified stichtite. However, the 1H cell cannot describe the positions of all reflections not accounted for by the $3R_1$ cell. The presence of *00l* reflections at $d = 10.7$ Å, 7.2 Å, 5.4 Å, and 3.6 Å suggests a three-layer periodicity with $c = 21.6$ Å. Reflections *100, 106, 118, 11.10,* and *304* at $d = 4.6$ Å, 2.85 Å, 2.203 Å, 1.681 Å, and 2.478 Å, respectively, violate rhombohedral symmetry and imply that the symmetry of the cell is 3H. The reflection at $d = 4.6$ Å can be indexed as *100* implying that *a* is $\sqrt{3}$ times greater than the basic periodicity of brucite-like layers. All experimental re-

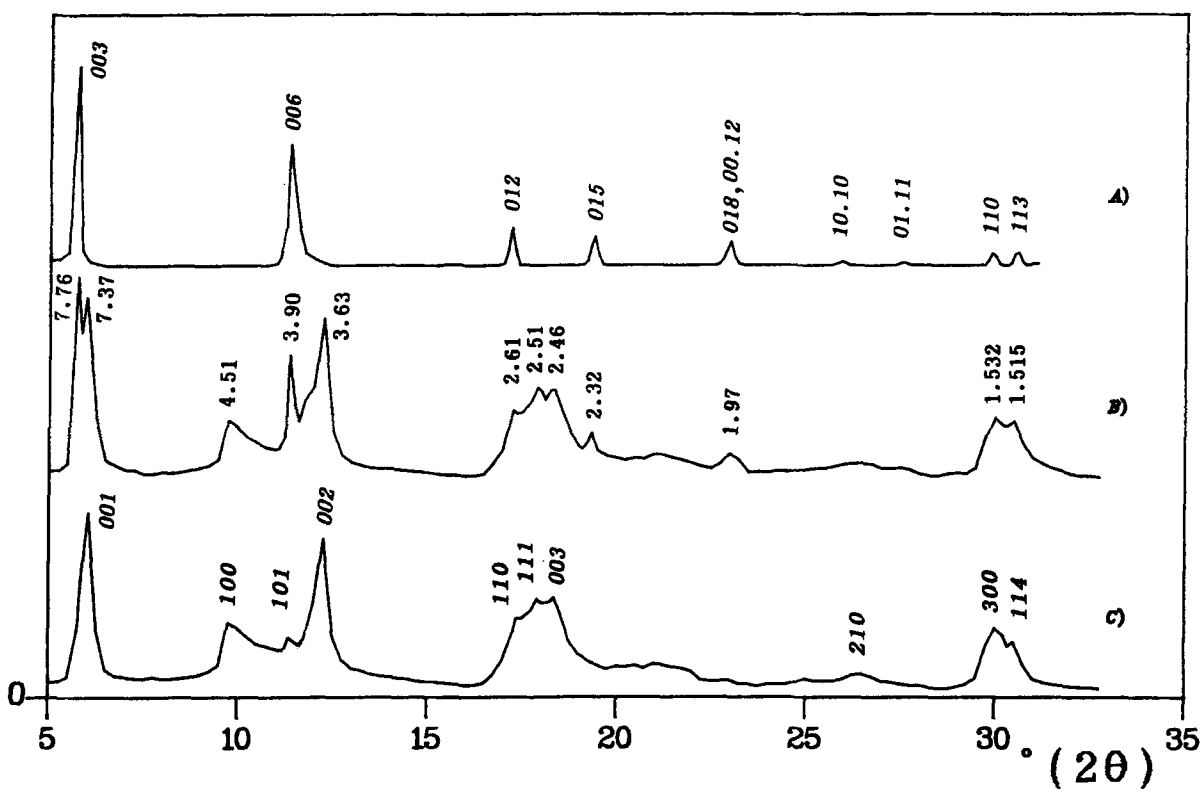

Figure 1. Experimental XRD patterns of the different fractions of a stichtite sample: A) = pink grains $3R_1$; B) = pink grains exposed to light; C) = greenish grains (modified stichtite 1H), Cu$K\alpha$ radiation.

Table 2. Experimental (exp) and calculated (cal) peak positions and intensities of stichtite.

Pink grains					Greenish grains		
hkl	d_{cal}[1] (Å)	d_{exp} (Å)	I_{cal} (%)	I_{exp}[2] (%)	*hkl*	d_{cal}[3] (Å)	d_{exp} (Å)
003	7.800	7.76	100	100	*001*	7.360	7.37
006	3.900	3.90	29	29	*100*	4.590	4.51
101	2.654	—	2	—	*101*	3.895	3.90
012	2.605	2.607	8	9	*002*	3.680	3.63
009	2.600	2.600	1	1	*110*	2.650	2.61
104	2.430	—	2	—	*111*	2.493	2.51
015	2.320	2.323	6	7	*003*	2.453	2.46
107	2.087	—	1	—	*210*	1.734	≈1.7
018	1.972	1.976	7	6	*300*	1.530	1.532
00.12	1.950	—	0	—	*114*	1.511	1.515
10.10	1.760	1.764	3	1			
01.11	1.664	1.667	2	1			
00.15	1.560	—	0	—			
110	1.542	1.545	4	3			
113	1.513	1.516	3	3			
10.13	1.493	1.496	1	1			
116	1.434	1.437	1	1			
10.14	1.417	—	1	—			
021	1.334	—	1	—			
202	1.327	1.330	1	1			
119	1.327	—	0	—			
024	1.302	1.303	0	1			
00.18[4]	1.300	1.303	1	1			
205	1.284	—	1	—			
10.16	1.283	1.283	1	1			

[1] a = 3.085 Å, c = 23.400 Å, $3R_1$.
[2] Intensities of basal reflections were measured on the diagram of oriented film and normalized to 100%. Intensities of other reflections were measured on the diagram of randomly oriented sample and normalized to the calculated pattern.
[3] a = 5.30 Å, c = 7.36 Å, 1H.
[4] Observed only for the oriented sample.

flections can be indexed in terms of $3R_1$ and 3H cells. The reevesite sample contains two phases: $3R_1$ reevesite proper and 3H modified reevesite.

The general mechanism for the formation of modified stichtite and modified reevesite is unclear. Hydrothermal syntheses of hydrotalcite-like compounds at elevated pressure (Pausch *et al.*, 1986) may provide a hint. The authors recorded the appearance of a poorly organized hydrotalcite-like material each time the temperature reached a limit that depended on the Mg-Al proportion. The material never appeared at atmospheric pressure. The XRD patterns contained all the important features seen in the pattern of greenish grains in our study, including a rational series of basal reflections with d = 7.4 Å and d = 3.71 Å; non-basal reflections at d = 4.57 Å and d = 1.68 Å; and two-dimensional diffraction bands. The authors interpreted the material as a transitional phase between three-layer hydrotalcite and two-layer manasseite. We would propose that it was a 1H mineral with $a \approx 5$ Å.

The principal conclusion of this paper is that both stichtite and reevesite do exist and are isostructural to

Table 3. New indexing of experimental peak positions on stichtite X-ray diagram.

hkl_{3R1}[1]	hkl_{1H}	$d_{1H\text{-}cal}$[2]	d_{exp}[3]
003			7.8
	001	7.280	7.2
	100	4.610	4.30
006	*101*	3.900	3.91
	002	3.640	3.62
	102	2.858	2.87
012			2.60
	111	2.502	2.50
015			2.32
018			1.97
	004	1.820	1.84
10.10			1.76
01.11			1.66
110			1.54
113			1.51
10.13			1.49
116			1.43
01.14			1.40
119			1.30
10.16			1.28

[1] Calculated d-values in $3R_1$ cell are listed in Table 1.
[2] a = 5.330 Å, c = 7.280 Å.
[3] Data from ASTM card # 14-330.

Table 4. New indexing of experimental peak positions on reveesite X-ray diagram.

hkl_{3R}	d_{cal}[1]	hkl_{3H}	d_{cal}[2]	d_{exp}[3]
		002	10.800	10.7
003	7.600			7.6
		003	7.200	7.2
		004	5.400	5.4
		100	4.623	4.6
		102	4.250	4.2
006	3.800			3.8
		006	3.600	3.61
		105	3.156	3.12
		007(?)	3.080	2.96
		106	2.840	2.85
		008	2.700	2.71
101	2.651	*110*	2.665	2.65
012	2.599			2.60
		113	2.503	2.51
104	2.417			2.416
015	2.303			2.301
		116	2.144	2.141
107	2.063			2.064
018	1.947			1.947
		118	1.898	1.903
		119	1.785	1.783
10.10	1.732			1.735
		11.10	1.679	1.681
01.11	1.636			1.636
110	1.541			1.541
113	1.510			1.510
		304	1.481	1.478
10.13	1.464			1.465
116	1.428			1.427

[1] a = 3.082 Å, c = 22.770 Å, $3R_1$.
[2] a = 5.337 Å, c = 21.600 Å, 3H.
[3] Data of De Waal and Viljoen (1971).

$3R_1$ hydrotalcite. Modified varieties of these minerals, which obviously cannot be attributed to the hydrotalcite-like family, may form *in situ*.

Geological Institute of the Russian Academy of Sciences A. S. BOOKIN
V. I. CHERKASHIN
109017 Moscow, Phyzevsky, 7 V. A. DRITS
Russia

REFERENCES

Allmann, R. and Jepsen, H. P. (1969) Die struktur des Hydrotalkites: *N. Jahrb. Mineral. Monatsh.* **1969,** 544–551.

Bookin, A. S. and Drits, V. A. (1993) Polytype diversity of the hydrotalcite-like minerals. Part I. Possible polytypes and their diffraction features: *Clays & Clay Minerals* (this issue).

De Waal, S. A. and Viljoen, E. A. (1971) Nickel minerals from Barberton, South Africa: IV. Reevesite, a member of the hydrotalcite group: *Amer. Mineral.* **56,** 1007–1088.

Pausch, I., Lohse, H.-H., Schurmann, K., and Allmann, R. (1986) Syntheses of disordered and Al-rich hydrotalcite-like compounds: *Clays and Clay Minerals* **34,** 507–510.

Tatarinov, A. V., Sapozhnikov, A. N., Prokudin, S. G., and Frolova, L. P. (1985) Stictite in serpentinites of Terektinsky ridge (Mountain Altay) (in Russian): *Zapisky Vsesouznogo Mineralogitcheskogo Obchestva* **114,** 575–581.

Taylor, H. F. W. (1973) Crystal structures of some double hydroxide minerals: *Mineral. Mag.* **39,** 377–389.

White, J. S., Henderson, E. P., and Mason, B. (1967) Secondary minerals produced by weathering of the Wolf Creek meteorite: *Amer. Mineral.* **52,** 1190–1197.

(Received 27 April 1992; accepted 25 March 1993; Ms. 2213c)